KSME

Springer

Journal of Mechanical Science and Technology 35 (12) 2021

Original Article
DOI 10.1007/s12206-021-1145-4

Keywords:
· Trapezoidal solar pond
· Mixture of salt solution
· Solar energy
· Energy efficiencies of solar pond

Correspondence to:
Dineshkumar P
dineshkumar@gcesalem.edu.in

Citation:
Dineshkumar, P., Raja, M. (2021). Experimental study on the thermal performance of a KNO_2-KNO_3 mixture in a trapezoidal solar pond. Journal of Mechanical Science and Technology 35 (12) (2021) 5765~5772.
http://doi.org/10.1007/s12206-021-1145-4

Received April 24th, 2021
Revised August 16th, 2021
Accepted August 17th, 2021

† Recommended by Editor
Tong Seop Kim

Experimental study on the thermal performance of a KNO_2-KNO_3 mixture in a trapezoidal solar pond

Dineshkumar P and Raja M

Department of Mechanical Engineering, Government College of Engineering, Salem - 636011, Tamilnadu, India

Abstract Salt gradient solar ponds (SGSPs) are thermal devices used for storing solar energy for low-temperature applications. The thermal performance analysis of an SGSP was investigated experimentally by artificially establishing a density gradient with sodium chloride (NaCl) and a mixture of potassium nitrite and potassium nitrate (KNO_2-KNO_3) solution under prevailing weather conditions in Salem, India. The solar pond was trapezoidal and constructed of plywood. The sides of the pond were completely covered with polythene sheets and given a black coating. The experiment was conducted over four months, and its thermal performance was noted. The outcomes of the experimental work showed that the solar pond with KNO_2-KNO_3 gives a temperature difference of approximately 35 °C between the lower convective zone (LCZ) and upper convective zone (UCZ) and observed maximum temperatures of 66 °C and 57 °C in the heat storage zone of the KNO_2-KNO_3 and NaCl solar ponds, respectively. Energy storage in the LCZ with KNO_2-KNO_3 was higher than that in the LCZ with NaCl, owing to the high-volume heat capacity of KNO_2-KNO_3, and the maximum temperature difference was approximately 9 °C. The energy efficiencies of the LCZ for NaCl and KNO_2-KNO_3 were 25 % and 33.5 %, respectively.

1. Introduction

The demand for power generation has increased due to population and industrial developments. Many countries are searching for alternatives to fossil fuels because of shortages. The use of renewable energy sources is the best alternative to depleting fossil fuels because they are imperishable, with zero or low emissions. Solar energy is used all around the world to meet the need for energy [1]. Therefore, an SGSP is a trouble-free and economic solar device that is used for storing solar energy by collecting solar insolation [2]. The stored heat energy is utilized for low-temperature applications [3].

An SGSP is a water body that captures and accumulates solar heat for long periods. Salinity profiles are developed by dissolving salts in water at distinct concentrations [4]. A solar pond mostly has three regions: an LCZ, a non convective zone (NCZ) and a UCZ. The topmost layer is the UCZ, which is commonly filled with freshwater periodically to maintain the stability of salt diffusion from the LCZ to the UCZ. The NCZ is established below the UCZ by having a linearly increasing salinity gradient. The formation of an NCZ will suppress the thermal convection heat loss from the LCZ. The LCZ of the solar pond plays an important role in storing solar energy. It is established at the bottom of the pond and has a constant and uniform density [5-7].

SGSPs have been extensively studied due to their excellent thermal energy collection and storage performances. Many researchers have theoretically and experimentally studied SGSPs to determine their working principles and performance. In this regard, the geometrical shapes of a solar pond can enhance thermal performance. A rectangular SGSP with an area of 4 m^2 and depth of 1.5 m was theoretically studied to assess the energy efficiency of the LCZ by using sodium chloride (NaCl). The results showed that the energy efficiencies were 11.38 %, 18.92 %

and 30.94 % for January, May and August, respectively [8]. In another work, a rectangular-shaped solar pond with a volume of 3.57 m^3 using sodium chloride (NaCl) was investigated experimentally and numerically in Jordan. From the experimental outcomes, it was observed that the maximum temperature of the LCZ was 46.9 °C [9].

A laboratory-scale solar pond with dimensions of 1 x 2 x 1 m^3 was studied experimentally. In this work, the maximum temperature was recorded to be 54 °C in the heat storage zone [10]. The performance of a small-scale prismatic solar pond with an area of 60 x 50 cm^2 and a depth of 60 cm with sodium carbonate (Na_2CO_3) was analyzed experimentally and numerically. Sodium carbonate was used to achieve a density gradient and could suppress convection thermal loss from the LCZ to the UCZ of the pond [11]. The temperature profiles of circular and rectangular solar ponds with similar cross-sections of 0.51 m^2 and volumes of 0.326 m^3 were compared experimentally by using NaCl. The maximum average temperature of a rectangular solar pond in the LCZ was recorded as 74 °C due to the smaller shadow region [12].

A trapezoidal solar pond with top surface area of 1.625 m x 1.625 m, a bottom surface area of 0.71 m x 0.71 m and a depth of 0.90 m was investigated for thermal performance experimentally. It was found that the trapezoidal solar pond had an 11 % more sunny region than a cuboid solar pond. This was due to the inclination of sidewalls, and a maximum temperature of 70.5 °C was recorded in the LCZ [13]. A trapezoidal SGSP with an area of 5.76 m^2 was investigated experimentally and numerically to study its temperature profile. From the experimental results, it was concluded that the temperature in the LCZ of the trapezoidal pond was approximately 5 °C higher than in a rectangular pool. It was found that the trapezoidal geometry helped to suppress the heat loss and turbidity between the UCZ and NCZ, which increased the stability of the pond [14].

The various parameters of a trapezoidal SGSP with a top surface of 2 x 2 m^2 and a bottom surface of 1 x 1 m^2 were investigated experimentally. It was concluded that the temperature of the LCZ reached 16.06 °C over a month comprising both sunny and rainy days [15]. A thermal energy analysis of a trapezoidal SGSP with a 2 m^2 surface area was performed numerically for steady temperature difference across the NCZ using a MATLAB code. It was found that thermal storage was significantly reduced in the solar pond by reducing the NCZ thickness [16]. The temperature distribution of the various zones of a trapezoidal SGSP was studied numerically by varying the thicknesses of the LCZ and NCZ. It was concluded that increasing the thickness of the LCZ and NCZ caused increases in the LCZ temperature of the pond [17].

Apart from geometrical shapes, the thermal performance can be increased by adding a porous medium or a phase change material (PCM) to the LCZ to suppress convection [18]. The thermal behavior of a circular-shaped solar pond with a PCM (paraffin wax) in the LCZ was investigated experimentally. It was found that the addition of a PCM increased the thermal and salinity constancy, which was at odds with the surrounding brawl and heat extraction [19]. An encapsulated PCM with nanoparticles in the heat storage zone of an SGSP was studied by experimentation. The addition of nanoparticles with a PCM contributed to storing more heat than in conventional solar ponds. After sunset, a higher water temperature was attained [20].

Several researchers have studied the thermal performance of various salts under solar and simulated conditions. From previous studies, it was observed that the generally used salt in solar ponds is NaCl. Apart from NaCl, other salts have also been investigated in terms of their preparedness to form salinity profiles. The temperature distribution and thermal stability of an SGSP were investigated experimentally by using ammonium sulfate ($(NH_4)_2SO_4$) instead of NaCl. It was found that $(NH_4)_2SO_4$ provides better thermal stability in the LCZ, achieving a maximum temperature of 83 °C [21]. In another work, ammonium salt was used to develop the salinity gradient, and its thermal performance was investigated experimentally. The results showed that the thermal performance of ammonium salt is analogous to that of NaCl and exhibits similar optical and thermophysical properties [22].

The salinity profile of a circular-shaped solar pond was developed by using magnesium chloride ($MgCl_2$), and the thermal performance was experimentally investigated. It was noted that stability and gradient layer stratification are attainable within a temperature range of 42 °C to 72 °C [23]. The development of salinity and temperature profiles for a mixture of 84 % carnalite ($KCl.MgCl_2.6H_2O$) and 16 % NaCl was studied experimentally. It was found that the steady state of the solar pond was achieved after five weeks of solar pond establishment [24]. A comparison between three solar ponds containing urea (NH_2CONH_2), NaCl and $MgCl_2$ was investigated experimentally. The results revealed that the temperature difference between the UCZ and LCZ was 23 °C, as measured by the 35 % salinity of urea [25]. Muriate potash (MOP) solar ponds were studied under simulated conditions between a temperature range of 40 °C to 70 °C by varying the heat input in the LCZ. It was found that the temperature drop of MOP in the LCZ was reduced when compared to NaCl and saltless ponds [26].

From the open literature, it can be observed that various salts, such as magnesium chloride, ammonium salts, urea, and carnalite mixed with sodium chloride, are suitable for developing a density gradient. However, SGSP salinity profiles with KNO_2-KNO_3 have not been tested. Solar ponds can take any geometrical shape. However, a trapezoidal shape is often preferred. The lateral walls of the solar pond constructed in this work are inclined to 45°, which increases the top surface area for receiving more solar irradiation and helps to reduce the shadow region in the LCZ. This slope also increases the salt concentration level at the bottom of the LCZ. Therefore, the trapezoidal geometry of solar ponds constructed in this work can enhance heat storage and thermal stability. The stored heat is utilized for low-temperature applications for a long period with low investments. Hence, the thermal behavior of a trapezoidal pond with

a KNO_2 - KNO_3 solution was examined. The outcomes of the experimental work are presented and discussed.

2. System description

2.1 Experimental setup

An experimental setup of two identical trapezoidal-shaped solar ponds was constructed with a depth of 30 cm, a top surface area of 65 × 65 cm, and a bottom area of 30 × 30 cm, which was located at the Government College of Engineering, Salem, Tamilnadu, India (11.7128° N latitude, 78.0882° E longitude). Schematic diagrams and photographs of the trapezoidal solar ponds are shown in Figs. 1 and 2. The ponds were fabricated using 18 mm thick plywood. Plywood is a good insulator due to its low thermal conductivity (0.13 W/m K). The inner sides of the bottom and lateral walls in the ponds were insulated using 2 mm thick polyurethane plastic with a bitumen coating to prevent water leakage. The coating was painted black to absorb more solar radiation. These ponds were placed on the top floor of the building to obtain maximum solar insolation.

The intensity of solar irradiation was measured using a CM 21 (Kipp & Zonen BV) precision pyranometer with an accuracy of ±1.5 W/m^2. The temperature profile of the various zones in the SGSP was measured by using six PT-100-type sensors with a ±0.5 °C accuracy. These six temperature sensors were placed vertically at a distance of 50 mm from the bottom of the pond. The temperature profile of the pond and ambient temperature were recorded by connecting the sensors using a 16-channel data acquisition system (Delphin EK make).

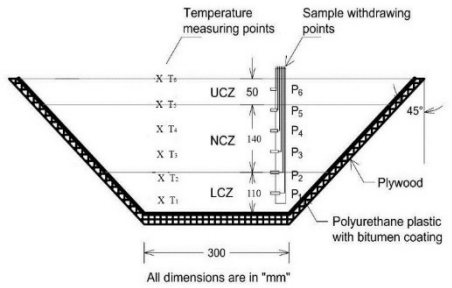

Fig. 1. Schematic diagram of trapezoidal solar pond.

Fig. 2. Photo of the experimental setup.

As stated by the principle of the SGSP, the assembly of each pond was split into a LCZ, NCZ and UCZ with thicknesses of 11 cm, 14 cm and 5 cm, respectively. An artificial salinity profile was created between the UCZ and LCZ. Initially, the LCZ of each pond was filled with the highest salinity brine solution. A linearly decreasing density profile was obtained from the top layer of the LCZ to form the NCZ. This was established by the slow pouring of the prepared brine solution layer by layer using a floating plastic can. Finally, with the addition of freshwater, the UCZ of each solar pond was established. The technique used to establish the salinity profile was similar to that delineated by the Kurt model [11]. A salt charger was installed in the lateral wall of each solar pond, as shown in Fig. 3. Periodically, salt was added to the salt charger of each solar pond. Due to mass transfer, salt diffusion occurs from the LCZ to the UCZ, which helps to maintain the thickness of the various zones in a solar pond. As the concentration of UCZ increased, fresh water was periodically added to the top of the UCZ.

The density of the brine solution was examined by taking small samples from the various zones of each solar pond. Flexible plastic tubes were fixed vertically at one side of the wall to take samples. The density of the taken samples in each solar pond was measured by weighing the mass of a given volume using a Sartorius B-310 digital scale with an accuracy of ±10^{-4} g. A 10 ml pycnometer with an accuracy of ±0.2 ml was used to measure the volume of the taken samples. Each pond was isolated for three days to achieve a linear salt gradient profile. The major parameters of the experimental setup are shown in Table 1.

After the establishment of a linear salt gradient, the temperature profile in the three zones of each SGSP, the intensity of solar radiation, and the ambient temperature were measured every hour from 6:00 to 18:00. The density levels were recorded once a day. The experiments were conducted separately using a NaCl solution and a KNO_2-KNO_3 solution with the same salt concentration from January to April 2020 under the meteorological conditions of Salem, Tamilnadu, India.

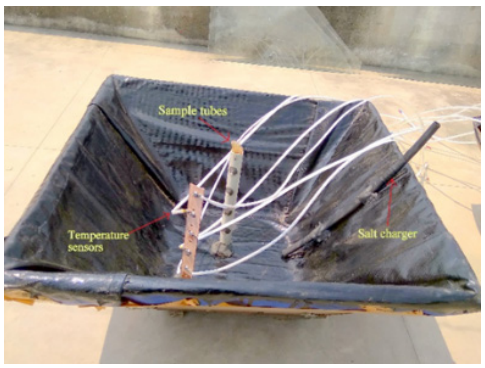

Fig. 3. Photo of the salt charger, temperature sensor and sample tubes.

Table 1. Details of experimental setup.

Sl. No	Parameters	Description
1	Solar pond	65 × 65 cm (top surface area), 30 × 30 cm (bottom surface area) and 30 cm (depth)
2	Material	Plywood (18 mm thick)
3	Inside solar pond	Insulated with 2 mm thick polyurethane plastic with bitumen coating
4	Pyranometer	Digital, CM 21 (Kipp & Zonen BV) with ±1.5 W/m^2 accuracy
5	Temperature	PT 100 type sensors (±0.5 °C accuracy), 6 numbers per solar pond
6	Data acquisition system	16 channel module with ±0.1 °C accuracy, Delphin EK make
7	Density measurement	Mass of sample was measured using B-310 digital scale with an accuracy of ±10^{-4} g. Volume as measured with 10 ml pycnometer to an accuracy of ±0.2 ml
8	Zone thickness	LCZ - 14 cm NCZ - 11 cm UCZ - 5 cm

Table 2. Comparison of present and Tahat model.

Model	Surface area (As)	Inclination of lateral wall
Tahat model [30]	1 m^2	45°
Present model	1.17 m^2	45°

2.2 Uncertainty analysis

The temperature distribution of the different zones of each solar pond was measured by using PT 100 temperature sensors with a range from -70 °C to 500 °C and an accuracy of ±0.5 °C. These temperature sensors were connected to a DAQ system for measuring the temperature in various zones, and their accuracy was 0.1 °C. By using the root sum of square methods [12], the total uncertainty in every measurement was calculated using Eqs. (1)-(4).

$$\Delta_{total} = \sqrt{\left(\Delta_{instrument}\right)^2 + \left(\Delta_{sensor}\right)^2} \quad (1)$$

$$\Delta_{instrument} = 0.101\ ^\circ\mathrm{C} \quad (2)$$

$$\Delta_{sensor} = \frac{0.5\ ^\circ\mathrm{C}}{\sqrt{3}} = 0.28 \quad (3)$$

$$\Delta_{total} = 0.38\ ^\circ\mathrm{C}\ . \quad (4)$$

2.3 Experiment validation

To validate the experimental results, the LCZ temperature of the solar pond with KNO_2-KNO_3 solution was compared under the summer climatic conditions in Salem with the calculated value of the Tahat model. The comparative parameters between the present and Tahat models are shown in Table 2.

According to the energy balance equation, the temperature of the LCZ was obtained [26].

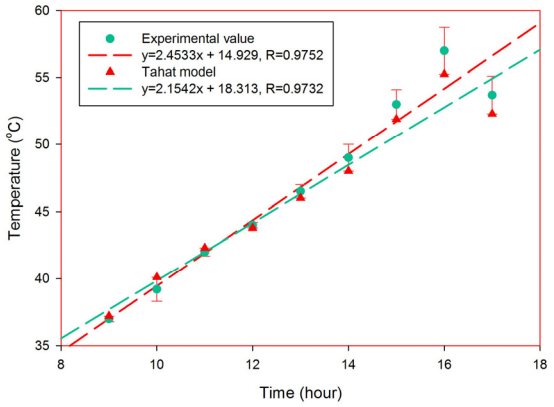

Fig. 4. Validation of the experimental setup with the Tahat model.

$$Q_{stored} = Q_{in} - Q_{loss} \quad (5)$$

$$T_{LCZ} = \frac{\left\{A_{sp}\left[h(x)I_r + \frac{k_w T_{atm}}{Z_{NCZ}}\right] + \frac{mC_p T_s}{\Delta t}\right\}}{\frac{mC_p}{\Delta t} + \frac{A_{sp}k_w}{Z_{NCZ}}} \quad (6)$$

where m is the quantity of water in the heat storage zone in kg, T_{atm} is the ambient temperature in K, I_r is the amount of solar radiation incident on the UCZ in W/m^2, k_w is the thermal conductivity of the brine solution in W/m K, Z_{ncz} is the depth of the NCZ in m, A_{sp} is the surface area of the pond in m^2, Δt is the time interval in secs, h(x) is the amount of solar intensity reaching depth x from the top surface, and C_p is the heat capacity of the brine solution in J/kg K. T_s is the storage zone temperature in K.

The experimental setup was validated using the three-day average temperature of the LCZ and compared with the Tahat model. Fig. 4 indicates that there is an acceptable consensus in the LCZ with a maximum error of 3.5 % between the experimental value and the Tahat temperature storage model, validating both the method and the experimental setup.

3. Energy analysis

An energy analysis is a viable tool for evaluating the thermal efficiency of processes and structures. In general, a solar energy system's energy analysis is used to assess energy production and losses to establish the necessary conditions for enhancing the system's efficiency. This can also provide a basic understanding of the SGSP and be used to predict the variations in thermal storage.

A profile of the temperature variations in the LCZ, NCZ and UCZ and the quantity of incident radiation accessing the top surface of the SGSP with ambient temperature and wind velocity were experimentally calculated. An energy study in the UCZ and NCZ was not performed owing to the low temperature. The maximum amount of useful thermal energy is stored in the LCZ of an SGSP [27, 28]. Therefore, heat fluxes in the LCZ were the main focus of this analysis. According to the conservation

of energy, the energy balance of LCZs can be written as follows.

$$\left(Q_{stored}\right)_{LCZ} = \left(Q_{solar} - Q_{loss}\right)_{LCZ} \tag{7}$$

where Q_{stored} is the total heat energy stored, Q_{loss} is the heat loss to the surroundings and Q_{solar} is the quantity of solar energy reaching the top surface of the LCZ as the energy input and is given by Mehmet Karakilcik [29] as follows.

$$\left(Q_{solar}\right)_{LCZ} = (1-a)(1-\beta)\,A_{LCZ} I_r e^{-\mu z} \tag{8}$$

where I_r is the amount of intensity of radiation entering the surface of the UCZ, a is the reflection factor of the pond's surface, β is the amount of solar irradiation arriving at the SGSP [30], A_{LCZ} is the normal area of the LCZ and μ is the absorption coefficient. For the present tests, a = 3-10 % and μ = 0.7 were used [11].

$$\beta = 1 - 0.6\left[\frac{\sin\theta_i - \sin\theta_r}{\sin\theta_i + \sin\theta_r}\right]^2 - 0.4\left[\frac{\tan\theta_i - \tan\theta_r}{\tan\theta_i + \tan\theta_r}\right]^2 \tag{9}$$

where θ_i is the angle of incidence and θ_r is the angle of refraction.

The experimental setup of each solar pond was constructed with plywood, which acted as an insulator. Therefore, the heat dissipation from the side and bottom walls of each SGSP occurred primarily in the heat transfer mode of conduction. Thus, the total heat loss in the LCZ was expressed in the Fourier law of conduction equation as follows.

$$\left(Q_{loss}\right)_{LCZ} = \left(Q_{up} + Q_{down} + Q_{side}\right)_{LCZ} \tag{10}$$

$$\left(Q_{loss}\right)_{LCZ} = \left[\frac{k_s}{x_{LCZ-NCZ}}\left(T_{LCZ} - T_{NCZ}\right)\right] + \left[\frac{k_{sw}}{x_s}\left(T_{LCZ} - T_{amb}\right)\right] + \left[\frac{k_{bw}}{x_b}\left(T_{LCZ} - T_{amb}\right)\right] \tag{11}$$

where Q_{up}, Q_{down} and Q_{side} are the cumulative heat losses to the surroundings from the thermal storage zone to the NCZ, downwall and sidewall of each solar pond, respectively, $x_{LCZ-NCZ}$ is the depth of the midpoints of the LCZ and NCZ, and x_s and x_b are the thicknesses of the side and bottom walls of each solar pond, respectively. T_{amb}, T_{LCZ} and T_{NCZ} are the temperatures of the ambient air, LCZ and NCZ, respectively.

The ratio of the usable energy stored to the amount of solar radiation reaching the LCZ of a solar pond is known as the energy efficiency. It can be expressed mathematically as follows.

$$\eta_{LCZ} = 1 - \frac{\left(Q_{loss}\right)_{LCZ}}{\left(Q_{solar}\right)_{LCZ}} \tag{12}$$

4. Results and discussion

In this study, two identical trapezoidal solar ponds with NaCl and KNO_2-KNO_3 were used to store thermal energy. In this work, the energy efficiencies of an SGSP with NaCl and an SGSP with KNO_2-KNO_3 were compared. The maximum amount of thermal energy was stored in the region of the LCZ compared with the other two zones of the pond; therefore, the energy efficiency of the LCZ was the focus [28, 31]. To minimize thermal convection heat losses from the heat storage zone, the stabilization of the density distribution of the SGSP is of considerable importance.

Figs. 5 and 6 depict the average experimental variation in the density distribution of each solar pond. Figs. 5 and 6 show that over time, mass diffusion occurred from the LCZ to the UCZ and increased the percentage of salinity in the UCZ because of evaporation in the UCZ. This was periodically mitigated by the addition of freshwater in the UCZ.

The temperature distribution of the three zones of each SGSP was measured using PT 100-type temperature sensors. Figs. 7 and 8 show the monthly average change in temperature for the NaCl and KNO_2-KNO_3 solar ponds over time during the test period. Temperature was measured at 13:00 for the respective depths, near the maximum temperature in the day. The monthly average ambient temperatures were 29 °C, 30.5 °C, 31 °C and 32 °C for January, February, March and

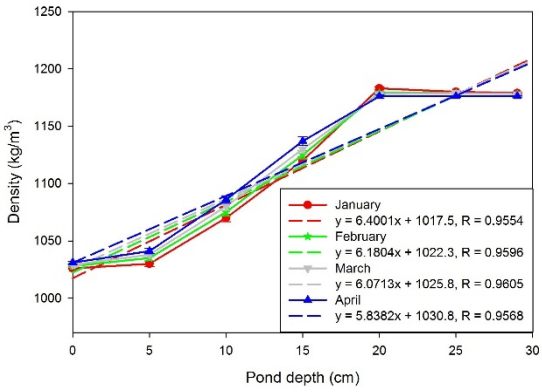

Fig. 5. Density distributions of the NaCl solar pond.

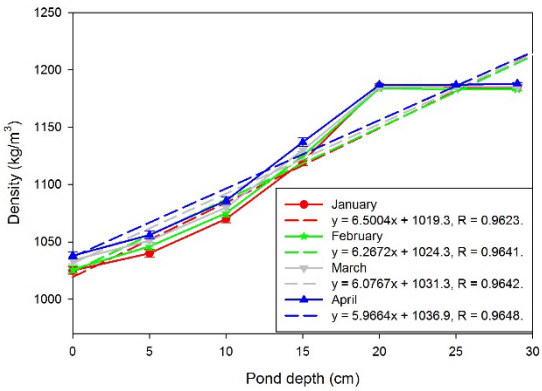

Fig. 6. Density distributions of the KNO_2-KNO_3 solar pond.

Table 3. Comparison of thermal properties of KNO_2-KNO_3 with other salts.

Salt	Thermal properties			
	Density (kg/m^3)	Heat capacity (kJ/kg K)	Thermal conductivity W/mK	Thermal diffusivity (m^2/s)
NaCl [31]	1200	3.28	0.58	1.47×10^{-7}
$CaCl_2$ [32]	1200	3.52	1.28	3.03×10^{-7}
$MgCl_2$ [33]	1200	3.50	0.61	1.45×10^{-7}
KNO_2 - KNO_3	1200	3.65	0.62	1.41×10^{-7}

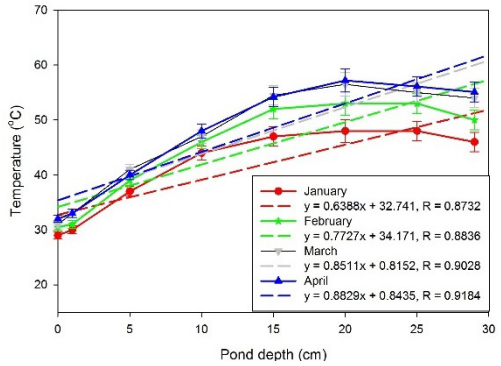

Fig. 7. Temperature profile of the NaCl solar pond.

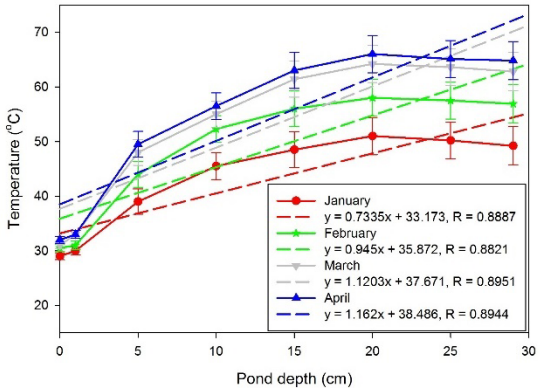

Fig. 8. Temperature profile of KNO_2-KNO_3 solar pond.

April, respectively. The temperature rose over time and reached a steady level approximately 12 weeks later, indicating that the lost and absorbed quantities reached equilibrium and that the solar pond reached stable operating conditions. It was observed that the maximum temperature occurred in the top layer of the LCZ and that the temperature decreased with increasing depth because of thermal convection due to the density difference.

Fig. 7 shows that the monthly average maximum and minimum temperatures were approximately 57 °C and 48 °C in April and January, respectively, for the NaCl solar pond. Similarly, Fig. 8 shows that the monthly average maximum and minimum temperatures were approximately 66 °C and 51 °C in April and January, respectively, for the KNO_2-KNO_3 solar pond. It was observed that KNO_2-KNO_3 showed a temperature rise that was approximately 15.79 % higher than that of NaCl and

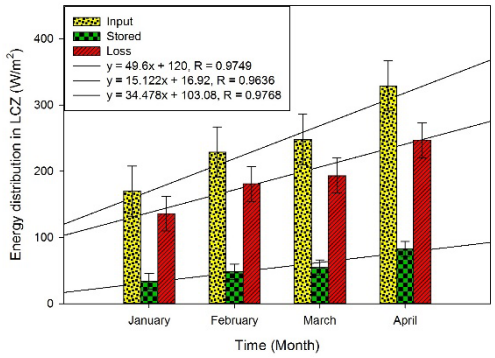

Fig. 9. Distribution of energy for the NaCl pond in LCZ.

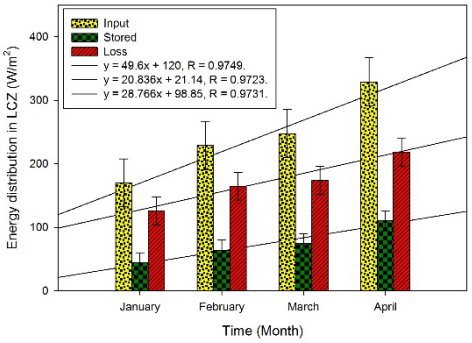

Fig. 10. Distribution of energy for the KNO_2-KNO_3 pond in LCZ.

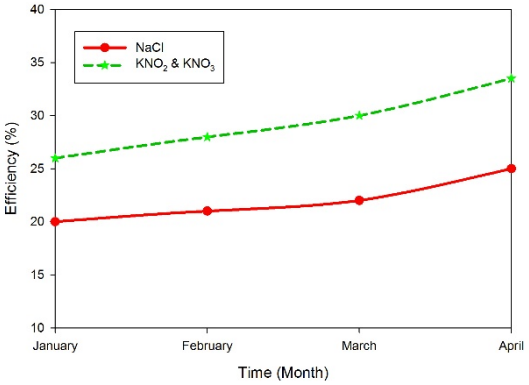

Fig. 11. The efficiencies of NaCl and KNO_2-KNO_3 solar ponds.

increased the stability of the LCZ.

In this study, the energy performance in the heat storage zone of the SGSP was calculated by using the intensity of ra-

diation reaching the top layer of the LCZ as the energy input and the energy losses stored in the LCZ. Figs. 9 and 10 indicate the energy variations of the NaCl and KNO_2-KNO_3 solar ponds, respectively, from January to April. As seen in Figs. 9 and 10, the heat energy stored in the LCZ of the SGSP reached a maximum of 82.25 W/m^2 and 110 W/m^2 in April and a minimum of 34 W/m^2 and 44 W/m^2 in January for the NaCl and KNO_2-KNO_3 solar ponds, respectively.

Fig. 11 indicates the variation in thermal energy storage efficiency for the LCZ of NaCl and KNO_2-KNO_3 solar ponds. Fig. 11 shows that a maximum energy efficiency of 33.5 % for KNO_2-KNO_3 and 25 % for NaCl was obtained in April. The experimental results indicate that the KNO_2-KNO_3 pond has better thermal storage than the NaCl pond. This is due to the high-volume heat capacity of KNO_2-KNO_3, which is used to enhance the thermal storage capacity of the SGSP. Table 3 shows the comparison of the thermal properties of KNO_2-KNO_3 with those of other salts.

5. Conclusion

In the present work, two distinct salts were used in two similar trapezoidal solar ponds to compare their thermal performances. From a previous study, it was observed that the maximum amount of energy is stored in the LCZ of an SGSP. Therefore, the experimental work carried out in this analysis concentrated on the LCZ of the pond. A density gradient was established artificially by using NaCl and KNO_2-KNO_3 separately in two similar trapezoidal solar ponds. The temperature profile, density distribution and energy storage efficiency of the SGSPs were investigated experimentally under prevailing weather conditions in Salem, India. The outcomes of the experimental work show the following:

- The maximum average temperatures were 57 °C and 66 °C for the NaCl and KNO_2-KNO_3 salts, respectively, in April. It was found that for KNO_2-KNO_3, the temperature rise was approximately 15.79 % higher than that of NaCl.
- The energy efficiency of the two salts in the LCZ was calculated using experimental parameters. It was found that the maximum energy of 82.25 W/m^2 and 110 W/m^2 were stored in the LCZ of NaCl and KNO_2-KNO_3 salts, respectively. Due to the high specific heat capacity of KNO_2-KNO_3, the salt energy storage efficiency was enhanced by 8.5 %. By comparison, the mixture of KNO_2-KNO_3 solar ponds stores more heat energy in the LCZ than the NaCl solar pond.

Nomenclature

A_s : Surface area of the solar pond
A_{LCZ} : Top surface area of the LCZ
a : Reflection factor of ponds surface
C_p : Thermal capacity of stored water
I : Amount of solar irradiation
k_w : Thermal conductivity of brine solution
Q_{stored} : Heat energy stored in LCZ
Q_{in} : Heat input
Q_{loss} : Heat losses
Δt : Time interval
Z_{ncz} : Height of NCZ

Greek symbols

μ : Absorption coefficient
η : Efficiency
β : Percentage of solar radiation at UCZ
θ : Angle

Subscripts

i : Incident
r : Refraction
sw : Sidewall
bw : Bottom wall

Abbreviations

DAQ : Data acquisition
LCZ : Lower convective zone
NCZ : Non convective zone
SGSP : Salt gradient solar pond
UCZ : Upper convective zone

References

[1] I. Dincer and A. Yapicioglu, *4.16 Solar Ponds*, Elsevier Ltd. (2018).
[2] A. Kasaeian, S. Sharifi and W. M. Yan, Novel achievements in the development of solar ponds: a review, *Solar Energy*, 174 (2018) 189-206.
[3] A. Abdulsalam, A. Idris, T. A. Mohamed and A. Ahsan, The development and applications of solar pond: a review, *Desalination and Water Treatment*, 53 (2015) 2437-2449.
[4] C. F. Kooi, The steady-state salt gradient solar pond, *Solar Energy*, 29 (1982) 177.
[5] C. Karim, S. M. Jomâa and A. Akbarzadeh, A laboratory experimental study of mixing the solar pond gradient zone, *Solar Energy*, 85 (2011) 404-417.
[6] A. H. Sayer, A. A. Monjezi and A. N. Campbell, Behaviour of a salinity gradient solar pond during two years and the impact of zonal thickness variation on its performance, *Applied Thermal Engineering,* 130 (2018) 1191-1198.
[7] F. Zangrando, A simple method to establish salt gradient solar ponds, *Solar Energy*, 25 (1980) 467-470.
[8] M. Aramesh, A. Kasaeian, F. Pourfayaz and D. Wen, Energy analysis and shadow modeling of a rectangular type salt gradient solar pond, *Solar Energy*, 146 (2017) 161-171.
[9] A. Sakhrieh and A. Al-Salaymeh, Experimental and numerical investigations of salt gradient solar pond under Jordanian climate conditions, *Energy Conversion and Management,* 65

(2013) 725-728.
[10] F. A. Banat, S. E. El-Sayed and S. A. El-Temtamy, Carnalite salt gradient solar ponds: an experimental study, *Renewable Energy,* 4 (1994) 265-269.
[11] H. Kurt, M. Ozkaymak and A. K. Binark, Experimental and numerical analysis of sodium-carbonate salt gradient solar-pond performance under simulated solar-radiation, *Applied Energy*, 83 (2006) 324-342.
[12] M. R. Assari, H. B. Tabrizi, A. K. Nejad and M. Parvar, Experimental investigation of heat absorption of different solar pond shapes covered with glazing plastic, *Solar Energy*, 122 (2015) 569-578.
[13] G. S. Dhindsa and M. K. Mittal, An investigation of double-glass-covered trapezoidal salt-gradient solar pond coupled with reflector, *International Journal of Green Energy*, 15 (2018) 57-68.
[14] H. Liu, L. Jiang, D. Wu and W. Sun, Experiment and simulation study of a trapezoidal salt gradient solar pond, *Solar Energy*, 122 (2015) 1225-1234.
[15] R. Goswami and R. Das, Investigation of thermal and electrical performance in a salt gradient solar pond, *Journal of Physics: Conference Series*, 1240 (2019).
[16] N.-U.-H. Shah, A. Arshad, A. Khosa, H. Ali and M. Ali, Thermal analysis of a mini solar pond of small surface area while extracting heat from lower convective layer, *Thermal Science*, 23 (2017) 166-181.
[17] A. M. A. Dayem and H. Shalaby, Numerical simulation of salt gradient solar ponds, *International Journal of Computational Engineering Science,* 5 (2004) 673-679.
[18] H. Wang, J. Zou, J. L. Cortina and J. Kizito, Experimental and theoretical study on temperature distribution of adding coal cinder to bottom of salt gradient solar pond, *Solar Energy,* 110 (2014) 756-767.
[19] M. R. Assari, H. B. Tabrizi and A. J. G. Beik, Experimental studies on the effect of using phase change material in salinity-gradient solar pond, *Solar Energy*, 122 (2015) 204-214.
[20] P. Sarathkumar, A. R. Sivaram, R. Rajavel, R. P. Kumar and S. K. Krishnakumar, Experimental investigations on the performance of a solar pond by using encapsulated Pcm with nanoparticles, *Materials Today: Proceedings*, 4 (2017) 2314-2322.
[21] J. R. Hull, D. L. Bushnell, D. G. Sempsrote and A. Pena, Ammonium sulfate solar pond: Observations from small-scale experiments, *Solar Energy*, 43 (1989) 57-64.
[22] J. R. Hull, Solar ponds using ammonium salts, *Solar Energy,* 36 (1986) 551-558.
[23] D. Subhakar and S. Srinivasa Murthy, Experiments on a magnesium chloride saturated solar pond, *Renewable Energy*, 1 (5) (1991) 655-660.
[24] S. H. Pawar and A. N. Chapgaon, Fertilizer solar ponds as a clean source of energy: Some observations from small scale experiments, *Solar Energy*, 55 (1995) 537-542.
[25] G. R. R. Murthy and K. P. Pandey, Comparative performance evaluation of fertilizer solar pond under simulated conditions, *Renewable Energy*, 28 (2003) 455-466.
[26] M. A. Tahat, Z. H. Kodah, S. D. Probert and H. Al-Tahaineh, Performance of a portable mini solar-pond, *Applied Energy*, 66 (2000) 299-310.
[27] M. Karakilcik, I. Bozkurt, I. Balkaya and I. Dincer, Investigation of heat storage performance of a solar pond with potassium chloride, *Progress in Clean Energy, Novel Systems and Application*, 2 (2014) 239-250.
[28] I. Bozkurt, S. Deniz, M. Karakilcik and I. Dincer, Performance comparison of sodium and magnesium chloride saturated solar ponds, *Progress in Clean Energy, Novel Systems and Application*, 2 (2014) 251-259.
[29] I. Bozkurt, S. Deniz, M. Karakilcik and I. Dincer, Performance assessment of a magnesium chloride saturated solar pond, *Renewable Energy*, 78 (2015) 35-41.
[30] M. N. A. Hawlader, The influence of the extinction coefficient on the effectiveness of solar ponds, *Solar Energy*, 25 (1989) 461-464.
[31] H. Wang, Q. Wu, Y. Mei, L. Zhang and S. Pang, A study on exergetic performance of using porous media in the salt gradient solar pond, *Applied Thermal Engineering* (2018) 301-308.
[32] M. Berkani, H. Sissaoui, A. Abdelli, M. Kermiche and G. Barker-Read, Comparison of three solar ponds with different salts throughbi-dimensional modeling, *Solar Energy,* 116 (2015) 56-68.
[33] I. Bozkurt, S. Deniz, M. Karakilcik and I. Dincer, Performance assessment of a magnesium chloride saturated solar pond, *Renewable Energy,* 78 (2015) 35-41.

P. Dineshkumar is a full time Ph.D. (Anna University, Chennai) scholar at Government College of Engineering, Salem in Department of Mechanical Engineering. He has received his B.E. degree from Mahendra Engineering College and M.E. degree from Government College of Engineering, Salem. His field of interest includes renewable energy, nanofluids and heat exchanger.

M. Raja is working as Assistant Professor in the Department of Mechanical Engineering, Government College of Engineering, Salem. He has received his B.E. degree from the Government College of Engineering, Salem and M. Tech. from the National Institute of Technology, Trichy. He pursued his Doctorate degree in area of heat transfer from Anna University, Chennai, India. His area of research includes renewable energy, Thermal Engineering, nanofluids and heat exchangers. He has more than 15 years of academic experience.